LUND UNIVERSITY

Photoionization-pumped gain at 185 nm in a laser-ablated indium plasma

Lacy, R. A; Nilsson, A. C; Byer, R. L; Silfvast, W. T; Wood, O. R; Svanberg, Sune

Link to publication

Total number of authors:
6

Photoionization-pumped gain at 185 nm in a laser-ablated indium plasma

R. A. Lacy,* A. C. Nilsson, and R. L. Byer

Department of Applied Physics, Stanford University, Stanford, California 94305

W. T. Silfvast and O. R. Wood II

AT&T Bell Laboratories, Holmdel, New Jersey 07733

S. Svanberg

Lund Institute of Technology, Department of Physics, P.O. Box 118, S-221 00 Lund, Sweden

We report what is to our knowledge the first production of gain by inner-shell photoionization of ions. Photoionization of $4d$ electrons from In$^+$ ions created a population inversion on a 185-nm In^{2+} transition. This scheme is an isoelectronic scaling of the 442-nm Cd$^+$ laser. A single-pass gain constant of 0.9 ± 0.3 cm^{-1} over a 0.4-cm path was pumped by soft x rays generated by less than 50 mJ of 1.06-μm light focused onto a tantalum target. Laser ablation of a liquid-indium target provided a high density (10^{16} cm^{-3}) of ground-state In$^+$ ions for this scheme. An indium amplified spontaneous emission laser and a synchronously pumped indium laser oscillator are proposed.

1. INTRODUCTION

We report what is to our knowledge the first production of gain by inner-shell photoionization of ions. Previous photoionization-pumped lasers, such as those described in Refs. 1 and 2, used gaseous neutral atoms as the medium to be pumped. Photoionization pumping of ions permits isoelectronic scaling of previously discovered lasers in order to obtain shorter wavelengths. The first photoionization-pumped laser was created in 1983 by Silfvast and co-workers[3] on 442- and 325-nm transitions of Cd$^+$. In this paper we describe the successful isoelectronic scaling of the visible Cd$^+$ 442-nm transition into the vacuum ultraviolet.

A single-pass exponential gain constant of 0.9 ± 0.3 cm^{-1} was obtained over a 0.4-cm path on the 185-nm In^{2+} $4d^95s^2$ $^2D_{5/2} \rightarrow 4d^{10}5p$ $^2P^\circ_{3/2}$ transition. Energy levels[4] for the indium gain scheme are shown in Fig. 1. The population inversion was created by photoionizing $4d$ electrons from ground-state In$^+$ ions, using broadband soft x rays in the 33- to ~150-eV range. These soft x rays were generated by the hot plasma resulting from focusing a ~50-mJ, 100-psec pulse from a 1.06-μm Nd:YAG laser onto a tantalum target at an intensity of ~10^{12} W/cm^2.

Based on gain measurements and gain modeling, we believe that a saturated-gain amplified spontaneous emission (ASE) laser at 185 nm could be produced by using only 0.5 J of 1.06-μm light in a 100-psec pulse for generation of the pumping soft x rays. A proposal is also presented for a synchronously pumped indium laser oscillator.

A crucial part of this work was the production and characterization of a dense plasma of In$^+$ ground-state ions. Laser ablation of a self-healing liquid-indium target provided the ions required for the gain scheme. A 100-mJ, 7-nsec pulse of 532-nm light, focused to an intensity of 5×10^8 W/cm^2 on the

indium target, produced a plasma containing primarily In$^+$ ground-state ions. For 400 nsec after ablation, more than 90% of the plasma consisted of In$^+$ ground-state ions at an ion density of greater than 10^{16} cm^{-3}. The laser ablation ion source is well suited for isoelectronically scaled short-wavelength laser schemes. It might also be useful for nonlinear-optics studies with ions.

2. THEORY

Duguay and Rentzepis[5] first proposed using inner-shell photoionization to produce population inversions on transitions of vacuum-ultraviolet and soft-x-ray wavelengths. Whereas photoionization cross sections for outer-shell electrons peak at threshold and decay rapidly with increasing energy, the cross sections of inner-shell electrons tend to be broad in energy. Furthermore, the inner-shell cross sections may be orders of magnitude greater than those of the outer shell. This makes ejection of an inner-shell electron more likely than outer-shell photoionization during illumination by broadband short-wavelength radiation. Thus broadband soft x rays emitted from a hot laser-produced plasma or a z-pinch plasma can efficiently and selectively populate a core-excited upper laser level by inner-shell photoionization.

Recalling Fig. 1, note that the ground state of the In$^+$ ion is isoelectronic to the ground state of neutral cadmium. As with cadmium, the photoionization of an inner-shell $4d$ electron from the In$^+$ ground state populates the core-excited $4d^95s^2$ ^2D term (the upper laser term) in the next higher ionization stage. Only one term, the $4d^{10}5p$ $^2P^\circ$, lies between the upper laser term and the $^2S_{1/2}$ ground state of In^{2+}, so the only radiative transitions available to the excited population are $4d^95s^2$ $^2D \rightarrow 4d^{10}5p$ $^2P^\circ$. The 185-nm $^2D_{5/2}$
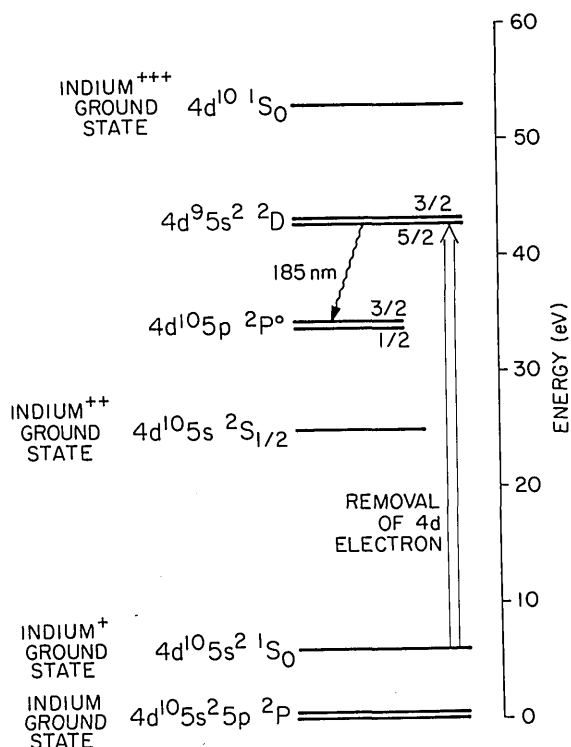
Fig. 1. Energy levels for photoionization-pumped 185-nm gain. The upper laser ^2D term is populated by photoionization of a $4d$ electron from a ground-state In$^+$ ion.

At present, the pumping efficiency for the indium laser scheme cannot be calculated, as the $4d$ and $5s$ photoionization cross sections for In$^+$ are not known. They should be similar to those of neutral cadmium, although shifted to higher energies. The In$^+$ $4d$ cross section has a threshold of 33 eV, as opposed to 18 eV for cadmium.[4] Measurements of the photoionization cross section for the $4d$ electron of neutral cadmium by Cairns *et al.*[8] show it to be $\sim$40 eV broad (FWHM) and to have a peak value of 14×10^{-18} cm^2 at 45 eV. It exceeds 10^{-18} cm^2 from 18 to well beyond 80 eV of photon energy. In contrast, the outer-shell $5s$ electron cross section of neutral cadmium peaks at only 0.27×10^{-18} cm^2 and has a FWHM of $\sim$1 eV. This disparity in behavior between the $4d$ and $5s$ cross sections makes selective inner-shell photoionization feasible with broadband radiation.

An important aspect of generating gain in a plasma expansion is the effect that the expansion has on the frequency profile of the path-integrated gain. Figure 2 shows the gain probe path broken up into small elements. We estimate that the 185-nm gain within each element had a Doppler profile with a FWHM of $\sim$10 GHz, corresponding to an ion temperature of $\sim$1 eV. Stark broadening of the 185-nm In^{2+} line at $n_e \sim 10^{16}$ cm^{-3} was negligible in comparison with thermal Doppler broadening, because of the high ionization stage and the lack of nearby levels that are dipole coupled to the upper laser state. In a simple model of the expanding plasma, the velocity of each element was assumed to be radially directed away from the ablation site, with constant magnitude independent of distance from the site. The line-center frequency of the gain within each element, as seen by a stationary observer viewing along the gain probe path, was Doppler shifted by the component of the expansion velocity in the direction of observation. These shifts caused the path-integrated gain to be spread over many thermal Doppler widths, resulting in low gain at the natural line center.

Figure 3 presents the calculated frequency profile of the path-integrated 185-nm gain under the conditions prevailing during the gain measurements described in Section 3. The density of ions in the upper laser level was assumed uniform throughout the plasma, and the plasma was assumed to be hemispherical in shape. These assumptions are consistent with our ion-density measurements and observa-

$\rightarrow$ $^2P^\circ_{3/2}$ transition is the best candidate for lasing, followed by the 153-nm $^2D_{3/2} \rightarrow ^2P^\circ_{1/2}$ transition. The 162-nm $^2D_{3/2} \rightarrow ^2P^\circ_{3/2}$ transition is weak compared with the other two. In the photoionization-pumped cadmium laser, the Cd$^+$ $^2D_{5/2} \rightarrow ^2P^\circ_{3/2}$ transition lased at 441.6 nm, whereas the same transition in In^{2+} occurs at 185.0 nm. The isoelectronic scaling from cadmium to indium more than doubles the photon energy for this $^2D_{5/2} \rightarrow ^2P^\circ_{3/2}$ transition.

The $4d^95s^2$ $^2D_{5/2} \rightarrow 4d^{10}5p$ $^2P^\circ_{3/2}$ laser transition is not dipole allowed in pure LS coupling; the oscillator strength comes from configuration interaction. For Hartree–Fock calculations, the eigenfunction of the upper level can be expanded in terms of pure LS-coupled states. The upper level (nominally $4d^95s^2$ $^2D_{5/2}$) contains small components of the pure LS configurations $4d^95p^2$, $4d^{10}5d$, and $4d^{10}6d$, which contribute oscillator strength for the transition to the $4d^{10}5p$ $^2P^\circ_{3/2}$ lower laser level. The lower level is relatively pure in LS coupling but contains some of the $4d^95s5p$ configuration, which contributes oscillator strength in the transition from the dominant $4d^95s^2$ configuration of the upper laser level to the lower laser level.

We calculated the emission oscillator strength f of the 185-nm In^{2+} $4d^95s^2$ $^2D_{5/2} \rightarrow 4d^{10}5p$ $^2P^\circ_{3/2}$ transition, using a Hartree–Fock code[6] with configuration mixing. Our calculated value is -0.006; we found no experimental values in the literature with which to compare this. However, comparison of a code calculation with the measured value of f for the 442-nm Cd$^+$ transition indicates that the calculated value of the 185-nm In^{2+} cross section may be low by a factor of $\sim$2. If so, the indium oscillator strength at 185 nm would be more than three times greater than the measured[7] -0.0035 oscillator strength of the isoelectronic 442-nm cadmium transition.
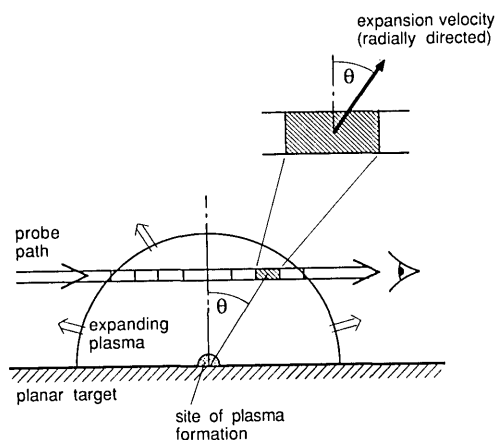

Fig. 2. Geometry of a gain probe path through an expanding plasma. The path-integrated gain was calculated by breaking the probe path into small elements, taking into account the position-dependent Doppler shifts caused by plasma expansion.
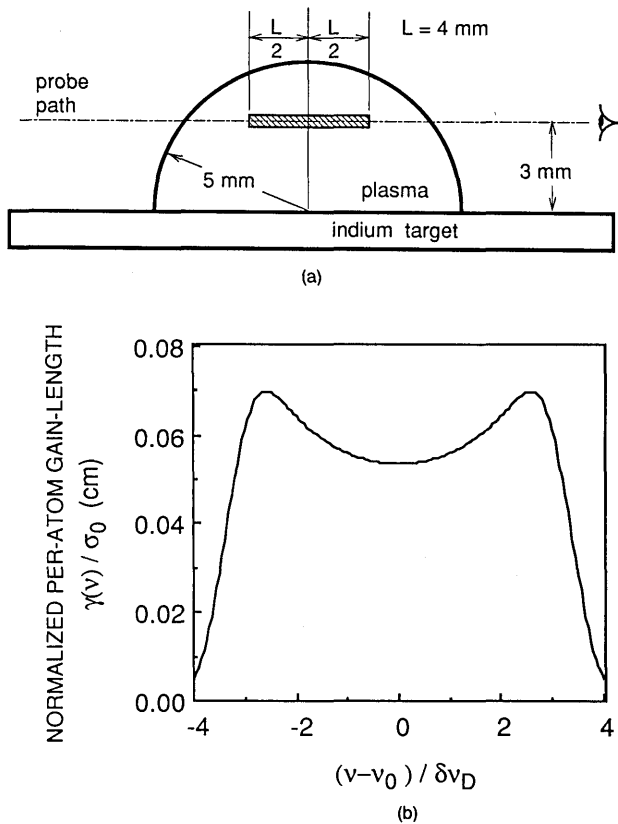
(a)

(b)

Fig. 3. Calculated frequency profile of 185-nm photoionization-pumped gain in a hemispherical indium-plasma expansion. Doppler shifts in the expanding plasma flatten the gain profile. (a) The shaded region is the intersection of the pumped region of the plasma with the small-diameter gain probe. (b) Path-averaged per-atom gain–length product γ versus frequency shift $(\nu - \nu_0)$ from natural line center ν_0, in units of thermal FWHM Doppler width $\delta\nu_D = 12$ GHz, corresponding to 1-eV ion temperature.

tions of emitted radiation from the plasma. At 445 nsec after ablation, when photoionization pumping was applied, the ablated indium plasma had expanded to a radius of 5 mm and had a measured radial expansion velocity of 1.3×10^6 cm/sec. Figure 3(a) indicates the gain probe path through the hemisphere of plasma, 3 mm above the indium target. The shaded region indicates the 4-mm segment of plasma that was x-ray pumped and provided gain. This segment was centered on the axis of symmetry of the hemisphere. In Fig. 3(b) the path-averaged per-atom gain–length product, γ, is shown as a function of frequency shift from natural line center. The ordinate is normalized to the single-atom 185-nm line-center Doppler-broadened gain cross section $\sigma_0 = 1.3 \times 10^{-14}$ cm^2. Intensity amplification is $\exp(\gamma N)$, where N is the excited-state density in units of inverse cubic centimeters.

Continuing the case of the previous paragraph, Fig. 4 shows the path-averaged gain–length product at natural line center, $\gamma(\nu_0)$, as a function of the length L of the pumped segment. At $L = 0.05$ cm, the Doppler shift occurring at each end of the pumped segment is equal to one FWHM thermal Doppler width; increasing the segment length L beyond this provides little increase in gain at natural line center. For comparison, the straight line shows the gain that would be obtained if Doppler shifts were not present.

The Doppler shifts caused by the hemispherical expansion of the plasma seriously distort the gain profile as a function of frequency, reducing the peak gain and increasing the difficulty of obtaining laser oscillation.

If the pumped path length is shorter than the total probe path through the plasma, as it was in our experiments, a higher peak gain can be obtain by pumping to one side of the
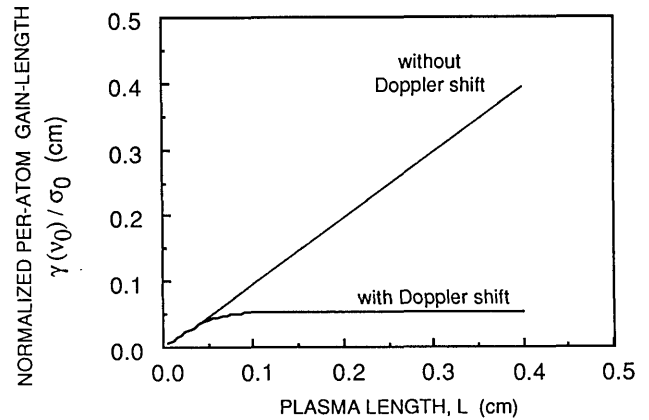
Fig. 4. Calculated path-averaged per-atom gain–length product γ at 185-nm natural line center ν_0, versus pumped path length in hemispherical plasma expansion. Conditions are the same as for Fig. 3.

(a)

(b)
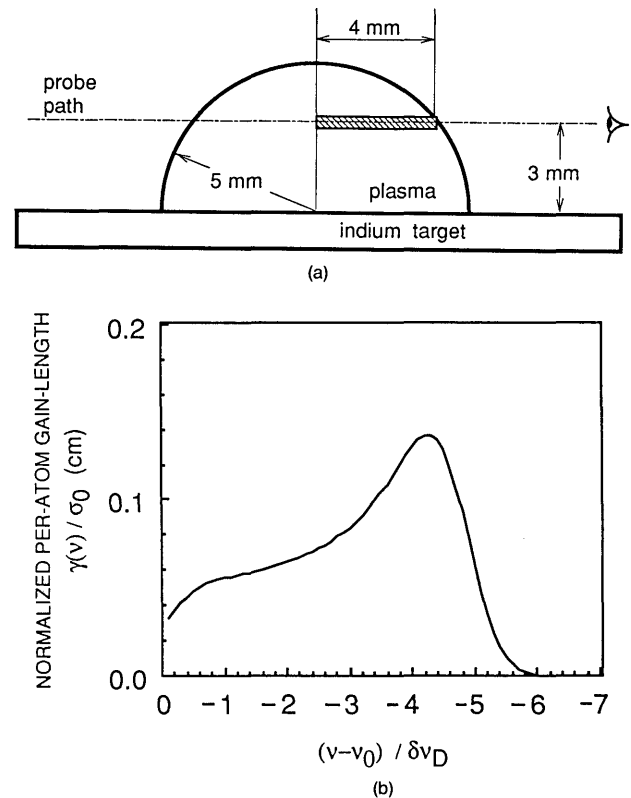
Fig. 5. Calculated frequency profile of 185-nm photoionization-pumped gain in a hemispherical indium plasma expansion; case of geometrically nonsymmetric pumping. (a) The shaded region is the intersection of the pumped region of the plasma with the small-diameter gain probe. (b) Path-averaged per-atom gain–length product γ versus frequency shift $(\nu - \nu_0)$ from natural line center ν_0, in units of thermal FWHM Doppler width $\delta\nu_D = 12$ GHz.

axis of symmetry of the hemispherical expansion, such that all the Doppler shifts are in the same direction. This situation is shown in Fig. 5, where a 4-mm segment of plasma to one side of the symmetry axis is pumped. The peak of the gain–length profile in Fig. 5 is greater than that obtained in the case of symmetric pumping shown in Fig. 3, although the same length of plasma is pumped. The rate of change of the Doppler shift, with respect to angle θ in Fig. 2, is $d\nu/d\theta \propto \cos(\theta)$ for $0 \leq \theta \leq 90°$; thus the gain peaks strongly at large θ. Nevertheless, the gain is still a factor of 3 times less than would be obtained if no Doppler shifts occurred.

The solution to the problem of Doppler shifts in the expanding plasma is to change the geometry of expansion. Focusing the ablation laser to a long, thin line instead of a large circular spot should generate an indium plasma that expands cylindrically. The cylindrical plasma will have no Doppler shifts in the direction of the axis of symmetry. This geometry is particularly well suited to creation of an ASE laser, since the long cylinder of plasma can be efficiently pumped by x rays generated by a line-focused laser, as demonstrated in Refs. 2 and 9. The requirements for a saturated-gain ASE laser are presented in Section 4.

3. EXPERIMENT

Ion-Density Measurements

Figure 6 shows the apparatus for ablating and x-ray pumping an indium plasma and for measuring the single-pass gain. To provide the In^+ ground-state ions for the gain scheme, indium was ablated with 67–100 mJ of 532-nm light in a 7-nsec pulse, focused to an intensity of $(1-5) \times 10^8$ W/cm^2 in a circular spot on the indium target. The indium target was kept liquid by an electrical heater and was thus self-healing. Helium at 2-Torr pressure filled the target chamber to reduce fouling of the windows.

Generally, ablation of a metal target with a Q-switched laser pulse at intensities of 10^8 to 10^{11} W/cm^2 initially creates a plasma of multiply ionized atoms that expands at ~10^7 cm/sec, producing a hollow expanding shell of ions.[10] After the laser pulse ends, a denser, cooler core plasma develops slowly at the ablation site, with evaporation from the target occurring for as long as several microseconds.[11] During the first

half microsecond after the laser pulse, electron-density measurements[10] reveal a roughly uniform density in the core. The core plasma expands at ~10^6 cm/sec. This core plasma was the source of In^+ ions for our experiment.

We determined time-resolved densities of the ground-state neutral and singly and doubly ionized indium atoms in the ablated indium core plasma by computer fitting of measured resonance-line absorption line shapes. The absorption line shapes were obtained with a scanning vacuum monochromator, using broadband vacuum-ultraviolet radiation from a laser-produced copper plasma to backlight the indium plasma. The copper plasma radiated strongly only during the laser pulse that generated it, providing time resolution of ~10 nsec for the density measurements. Also, time-dependent expansion velocities of the indium core and shell plasmas were measured. Details of the plasma diagnostics were presented in Ref. 12. The results pertinent to the production of gain by photoionization pumping are summarized below.

Our diagnostics on an ablated indium plasma were for the case of ablation with a 100-mJ, 7-nsec FWHM pulse of 532-nm light, focused to an intensity of 5×10^8 W/cm^2. The radius in millimeters of the resulting core plasma, assumed hemispherical in shape, was $r_{mm} = 0.0047(t_{ns})^{1.14}$, for time t_{ns} in nanoseconds, spanning 300 to 1000 nsec after ablation. The shell plasma, whose motion was retarded by the helium gas in the cell, had a radius $r_{mm} = 0.1(t_{ns})^{0.7}$. We believe that the shell plasma swept most or all of the helium ahead of it, allowing the core plasma to expand freely into a near vacuum, as evidenced by the positive acceleration ($d^2r/dt^2 > 0$) of the core boundary.

Within the core plasma, the density of In^+ $^1S_0$ ground-state atoms was $n^+(t) = 3.7 \times 10^{24}(t_{ns})^{-3.05}$ cm^{-3}, where time t_{ns} is in nanoseconds, based on measurements from 300 to 1500 nsec after ablation. The density of ground-state neutral indium atoms ($^2P^o_{1/2,3/2}$) was $n^o(t) = 6.0 \times 10^{21}(t_{ns})^{-2.28}$ cm^{-3}, based on measurements from 300 to 2000 nsec after ablation. In these density expressions of form $n = a(t)^b$, systematic error bounds for the linear coefficients a are estimated to be (+70%, −33%) for $n^+(t)$ and (+400%, −56%) for $n^o(t)$, owing to uncertainty in the calculated Stark broadening coefficients used to reduce the data. Systematic error
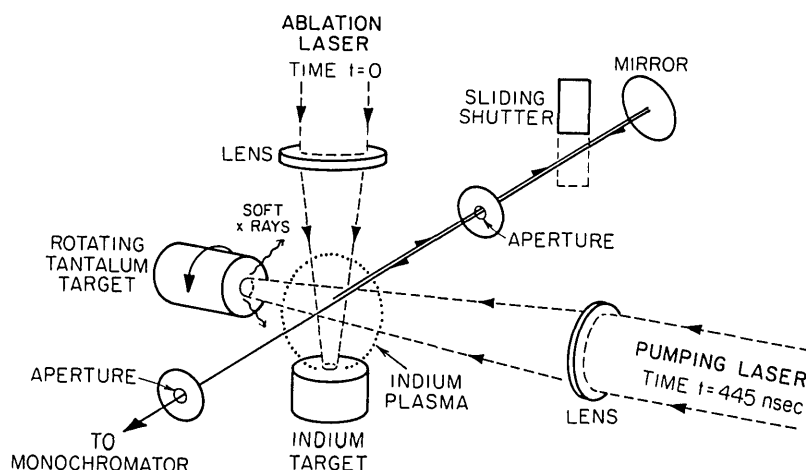

Fig. 6.   Apparatus for soft-x-ray excitation of a laser-ablated indium plasma. The single-pass gain is determined from the amplification of plasma light that has been reflected back through the plasma by a planar mirror.
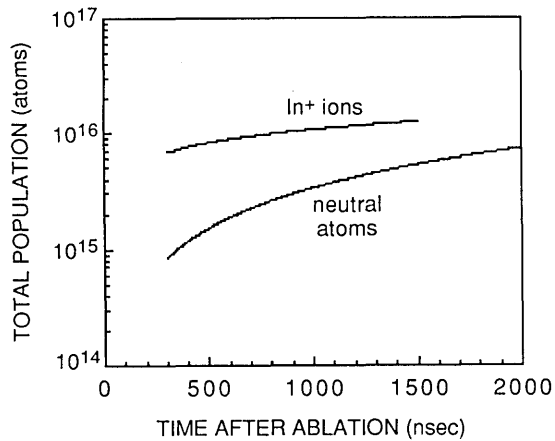
Fig. 7. Measured total number of ground-state atoms of neutral and singly ionized indium in the core of a laser-produced plasma.
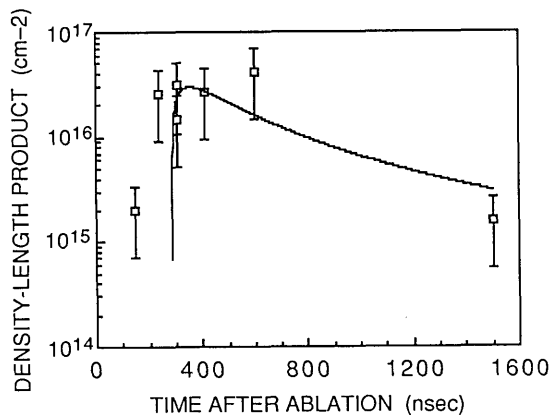

Fig. 8. Comparison of optical absorption measurements of the In$^+$ $^1S_0$ ground-state ion density–length product with a model of a uniform-density hemispherically shaped expanding plasma. Data suggest a diffuse boundary for the core plasma, compared with the infinitely sharp boundary of the model.

from the Stark coefficient uncertainty does not affect the exponential coefficients b.

Figure 7 shows the measured total number of ground-state neutral-indium and ground-state In$^+$ ions in the core plasma as a function of time. The populations grew with time because of continued evaporation of the target after the end of the ablating laser pulse.[11] For 400 nsec after ablation, ground-state singly ionized atoms constituted greater than 90% of the laser-ablated indium core plasma, with neutral atoms making up the balance. The population of doubly ionized indium in the core plasma was negligible. The low electron temperature of this plasma (we estimate <1 eV) ensured that only a fraction of a percent of the ions were thermally excited out of their ground state.

Figure 8 shows the measured time-dependent density–length product for ground-state In$^+$ ions along an optical path parallel to, but 3 mm above, the indium target face. This is the same optical path that was probed during the gain measurements described below (and shown in Figs. 6 and 9), so this density–length product is a measure of the total amount of In$^+$ ions present along the gain probe path before x-ray pumping. The individual data points were obtained by optical absorption measurements as noted

above. The solid curve in Fig. 8 is a model of the expanding core plasma, constructed from the measured time-dependent expansion velocity and ion density of the core plasma. The sharp peak in density–length product is due to the rapid expansion of the plasma and consequent reduction of density, not to loss of ions owing to recombination. In the model, the peak density–length occurred near 350 nsec after ablation, which should be the time at which to photoionization-pump the plasma to obtain the highest possible gain along this optical path. The In$^+$ density at this time was 4×10^{16} cm^{-3}, and the gain probe path length through the core plasma was 0.45 cm.

Gain Measurements

During the gain measurements, only 67 mJ of 532-nm light, focused to $\sim 1 \times 10^8$ W/cm^2, were used for indium ablation. A different laser and optical train were used for ablation in the gain measurements from those used during the density measurements. The ablation laser beam quality was poorer in the gain measurement setup, necessitating lower ablation intensity to avoid splashing of the liquid indium owing to high pressure at beam hot spots. Thus the ground-state In$^+$ ion density–length during gain measurements was likely less than that shown in Fig. 8. Also, we could not synchronize the ablation laser and the pumping laser to pump earlier than 445 nsec after ablation, although the model curve in Fig. 8 indicates that a smaller delay might have marginally improved the gain. It was observed qualitatively that the gain at 185 nm increased as the time delay between ablation
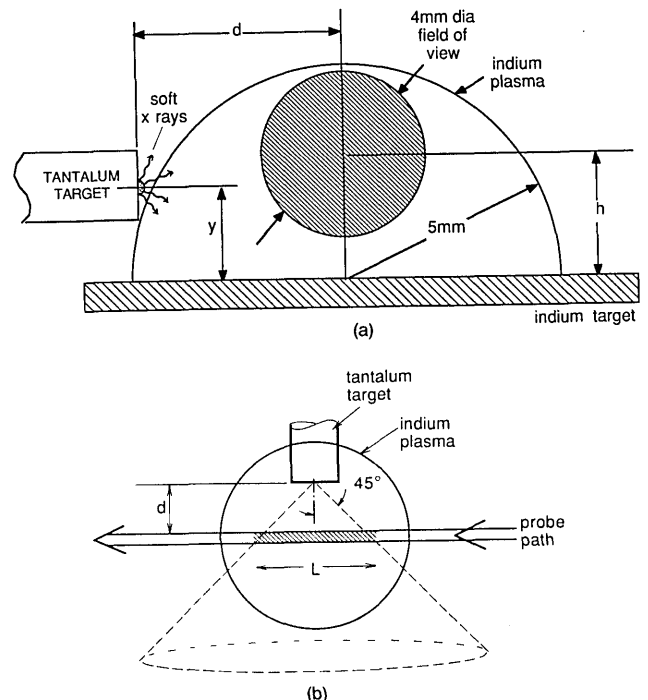
Fig. 9. Geometry of x-ray source, plasma expansion, and gain probe path. (a) View of hemispherical indium plasma, as seen from the monochromator during gain measurements (i.e., side view). The circle indicates the 4-mm-diameter field of view of the indium plasma seen by the monochromator. (b) Top view. Soft x rays from the tantalum plasma strongly pump the indium plasma within a cone of half-angle 45°. The shaded region shows the overlap of the pumped plasma and the gain probe beam.

and pumping was decreased to the minimum achievable delay of 445 nsec.

The pumping x rays were generated with ~50-mJ, 70–100-psec-long pulses of 1.06-μm light, focused onto the end face of a tantalum cylinder at an intensity of ~10^{12} W/cm^2. The tantalum target was rotated to reduce erosion. Short pump pulses were used so the soft-x-ray excitation would occur in a time short compared with the quenched gain lifetime, observed to be ~3 nsec.

Figure 9(a) shows the relative positions of the soft-x-ray source, the ablated indium plasma, and the 4-mm-diameter field of view of the monochromator that defined the region of the plasma in which gain was measured. The indium plasma had a 5-mm radius at the time of pumping, 445 nsec after ablation. The distance d from the x-ray source to the center of the probed region was varied between 2 and 5 mm, with best results at 2 mm. The distance h from the indium target to the axis of observation was 3–3.5 mm. The vertical position y of the x-ray-emitting plasma was adjusted for maximum gain; this position was not measured but is presumed equal to h.

For $d = 5$ mm, the largest single-pass intensity amplification observed was 1.31 ± 0.13, corresponding to a path-averaged exponential gain constant of 0.4 ± 0.15 cm^{-1} over a path length L of 0.7 cm. For $d = 2$ mm, the largest single-pass intensity amplification observed was 1.44 ± 0.14, corresponding to a path-averaged exponential gain constant of 0.9 ± 0.25 cm^{-1} over a path length L of 0.4 cm. Further gain data appear in Chap. 3 of Ref. 12, while App. E of that reference contains the detailed derivation of the data analysis formulas and the associated error analysis.

The pumped path length L was determined by the Lambertian intensity distribution[13] of the plasma x-ray source. Taking into account the decrease in x-ray flux with the square of the distance from the source, but ignoring pump depletion, this type of source effectively pumps a cone of half-angle $\theta = 45°$, as illustrated in Fig. 9(b). Pump depletion was not strong in this experiment. Assuming a maximum photoionization cross section of 14×10^{-18} cm^2 for the In$^+$ ions, and an ion density of 3×10^{16} cm^{-3}, the $1/e$ penetration depth of the x rays into the indium plasma was 2.4 cm.

Single-pass gain at 185 nm was determined by using a plane mirror to reflect light from the indium plasma back through the plasma and into a monochromator as shown in Fig. 6. A shutter was used to block and unblock the mirror; the ratio of the fluorescent intensity at the monochromator with the mirror unblocked to that with the mirror blocked was related to the single-pass gain of the plasma. To reduce the shot-to-shot variations in gain, a boxcar integrator performed a running average over 30 laser shots, while the shutter was repeatedly opened for several hundred laser shots and then closed for several hundred shots. The mirror reflectivities at 185 nm were checked with a vacuum reflectometer before and after the gain measurements to ensure that no degradation occurred from target debris. Two different mirrors were used during the 185-nm gain measurements: a 78% reflecting aluminum mirror with a MgF$_2$ overcoat and a 63% reflecting dielectric-coated mirror.

A Brewster-angle MgF$_2$ window separated the target chamber from a 0.5-m Seya–Namioka vacuum monochromator. A second Brewster-angle MgF$_2$ window was used in the early gain measurements to protect the mirror from target debris but was found unnecessary because of the 18-cm distance between plasma and mirror and was removed for later measurements. The polarization-dependent loss anisotropy introduced by the Brewster windows was included in the gain calculations.[12]

The validity of the single-mirror method of gain measurement was tested by pumping the indium plasma weakly, so that fluorescence at 185 nm was generated, but no measurable gain or loss was expected. The measured ratio of intensities at 185 nm with the mirror blocked and unblocked agreed with the predicted value within 3%. Another test of this method was reported in Ref. 14, in which good agreement was obtained between gain measurements of photoionization-pumped argon using the single-mirror technique and using a cw argon-ion laser to probe the gain. The photoionization-pumped argon-plasma electron density of ~10^{15-16} cm^{-3} was comparable with that in the indium experiment.

The $1/e$ decay lifetime of the photoionization-pumped 185-nm fluorescence was ~3 nsec, measured using a monochromator with a microchannel plate detector having subnanosecond resolution. This fluorescence lifetime was assumed exponential, although multiple-shot-exposure photographs of the weak oscilloscope trace of the decay curve did not resolve the curve well enough for certainty. The calculated natural fluorescence lifetime was 90 nsec, but, in the plasma, electron-collisional deexcitation of the $4d^9 5s^2$ $^2D_{5/2}$ upper laser state to the $4d^{10} 5p$ $^2P^\circ_{3/2}$ lower laser state shortened the upper-state lifetime. At 445 nsec after ablation, when pumping occurred, the electron density in the plasma was ~3×10^{16} cm^{-3}, and the electron temperature T_e was ≤ 1 eV. Given also our calculated emission oscillator strength $f = -0.006$, McWhirter's formula[15] for the collisional deexcitation rate yields an upper-state lifetime of ≤ 6 nsec. Electron-collisional excitation from the upper laser level to higher levels should be small compared with deexcitation because of the low plasma temperature. Although hot photoelectrons from the pumping process can cause collisional excitation out of the upper state, the density of photoelectrons was only a few percent that of the original cold-plasma electrons. Thus we expect the collisional excitation rate to be small compared with the deexcitation rate.

4. DISCUSSION

The measured single-pass amplifications and gain constants reported above are conservative values, as they were not corrected for the significant time delay between the soft-x-ray pumping and the reflection of plasma light to probe the gain. The path from the plasma to the mirror and back again was 42 cm, causing a delay of 1.4 nsec between the production of the population inversion and the subsequent probing of the gain. Because of the 3-nsec decay constant of the 185-nm photoionization-pumped fluorescence, the peak gain at the instant of pumping was a factor of 1.6 times larger than that revealed by the delayed probe.

One method to make a 185-nm laser would be to use high peak gain to achieve gain saturation by ASE. The measured gain of 0.9 cm^{-1} at 1.4 nsec after pumping should be increased by at least a factor of 3 by the elimination of Doppler shifts, as described in Section 2 above. Also, considering the

factor-of-1.6 increase in the peak gain over the gain measured at 1.4 nsec after pumping, a peak gain of ≥ 4 cm^{-1} should be achieved by eliminating Doppler shifts, if all other conditions are the same as in the experiments reported.

The expansion-induced Doppler shifts should be eliminated by focusing the indium ablation laser into a long, thin line on the target. The resulting indium plasma will expand cylindrically, with no component of velocity along the axis of symmetry. This geometry is ideal for producing a 185-nm saturated-gain ASE laser. Based on the ion-population measurements reported in Section 3, ablation of indium with ~1 J of 532-nm light in a 7-nsec pulse, focused to a rectangular spot of 0.06 cm × 5 cm at an intensity of ~5×10^8 W/cm^2, would produce 10^{17} ground-state In$^+$ ions in a cylindrically expanding plasma. Assuming that the plasma is uniform and is a cylinder of half-circular cross section, a density of 3 $\times 10^{16}$ cm^{-3} In$^+$ ground-state ions would occur when the cylinder radius reaches 0.65 cm. The 0.65 cm × 5 cm cylinder of ablated indium plasma would be pumped with the soft x rays generated from ~0.5 J of 1.06-μm light in a 100-psec pulse, focused in a 4-cm-long line onto a tantalum target at ~10^{12} W/cm^2. This should result in a 4-cm-long gain region with 4 cm^{-1} of gain, yielding an amplification of exp(16) along the axis of symmetry of the plasma cylinder. The full length of the indium plasma cylinder would not be pumped, because expansion parallel to the axis of symmetry will occur at the ends.

Of course, true laser oscillation is not achieved in an ASE laser. The fundamental problem with the indium scheme, common also to other short-wavelength lasers, is the collisionally reduced gain lifetime, which is too short for oscillation to build up between mirrors spaced far enough apart (~30 cm) to prevent damage from the plasma.

To overcome the lifetime problem, we propose to place the indium-plasma gain medium in an optical cavity and repetitively x-ray-pump the indium plasma at time intervals synchronized to the round-trip cavity period. True laser oscillation would be achieved by this method. An injection-seeded, Q-switched Nd:glass-slab regenerative amplifier being developed at Stanford University[16] will provide a string of ~9 pulses of 200 mJ each, spaced 5.8 nsec apart. This pulse train should generate soft-x-ray pulses of sufficient strength to drive a synchronously pumped 185-nm indium laser oscillator. Only a single laser pulse is needed for the indium ablation in this scheme, because the lifetime of the ablated In$^+$ plasma far exceeds the total 50-nsec pumping time.

Our calculations indicate that population buildup will not occur in the lower laser level because of this repetitive pumping scheme. The lower laser level ($5p$ $^2P^{\circ}_{3/2}$) has a dipole-allowed emission oscillator strength of $f = -0.27$ connecting it to the $5s$ $^2S_{1/2}$ ion ground state, based on the measured lifetime of 1.45 ± 0.1 nsec by Anderson *et al.*[17] for this 162.5-nm transition. In a plasma with $n_e = 3 \times 10^{16}$ cm^{-3} and $T_e = 1$ eV, McWhirter's formula for electron collisional deexcitation of the lower laser level to the ground state predicts a population decay time constant of 0.16 nsec, much shorter than the time between x-ray-pump pulses. The collisional excitation rate from the ground state to the lower laser level is 10^3 times smaller than the deexcitation rate. The collisional deexcitation of the lower laser level also prevents a

bottleneck due to radiation trapping in the dense plasma gain medium.

5. CONCLUSION

We obtained a gain constant of 0.9 ± 0.3 cm^{-1} over a 0.4-cm path at 185 nm by inner-shell photoionization of In$^+$ ions. This was an isoelectronic scaling of the visible 442-nm cadmium laser to a vacuum-ultraviolet wavelength. Less than 50 mJ of 1.06-μm light was required to generate the soft x rays, by way of a laser-produced plasma, for the photoionization pumping. Gain modeling indicates that a gain constant of 4 cm^{-1} can be obtained with the same x-ray-pumping flux and indium-ion density by changing the expansion geometry of the laser-ablated indium plasma. An indium ASE laser and a synchronously pumped indium laser oscillator were proposed and could be driven by laboratory-scale pump lasers.

We found laser ablation to be excellent for generating dense, cool, long-lived plasmas of ground-state singly ionized atoms. These plasmas are useful for short-wavelength photoionization-pumped lasers. They might also find use in nonlinear frequency generation.

REFERENCES

1. W. T. Silfvast and O. R. Wood II, "Photoionization lasers pumped by broadband soft-x-ray flux from laser-produced plasmas," J. Opt. Soc. Am. B **4**, 609–618 (1987).
2. H. C. Kapteyn, R. W. Lee, and R. W. Falcone, "Observation of a short-wavelength laser pumped by Auger decay," Phys. Rev. Lett. **57**, 2939–2942 (1986).
3. W. T. Silfvast, J. J. Macklin, and O. R. Wood II, "High-gain inner-shell photoionization laser in Cd vapor pumped by soft-x-ray radiation from a laser-produced plasma source," Opt. Lett. **8**, 551–553 (1983).
4. C. E. Moore, *Atomic Energy Levels* (National Bureau of Standards, Washington, D.C., 1971), Vol. III, pp. 55–72.
5. M. A. Duguay and P. M. Rentzepis, "Some approaches to vacuum UV and x-ray lasers," Appl. Phys. Lett. **10**, 350–352 (1967).
6. R. D. Cowan, computer codes RCN MOD 31 and RCG MOD 8 (Los Alamos Scientific Laboratory, Los Alamos, New Mexico).
7. Ya. F. Verolainen and V. I. Privalov, "Radiation lifetimes of ^2P and ^2D states in Cd II," Opt. Spectrosc. (USSR) **48**, 245–247 (1980).
8. R. B. Cairns, H. Harrison, and R. I. Schoen, "Photoionization with atomic beams. II. Cadmium atoms between 8.99 and 83 eV and zinc atoms between 27.35 and 65 eV," J. Chem. Phys. **51**, 5440–5443 (1969).
9. Guang-Yu Yin, C. P. J. Barty, D. A. King, D. J. Walker, S. E. Harris, and J. F. Young, "Low energy pumping of a 108.9-nm xenon Auger laser," Opt. Lett. **12**, 331–333 (1987).

10. P. T. Rumsby and J. W. M. Paul, "Temperature and density of an expanding laser produced plasma," Plasma Phys. **16,** 247–260 (1974).

11. F. J. Allen, "Production of high-energy ions in laser-produced plasmas," J. Appl. Phys. **43,** 2169–2175 (1972).

12. R. A. Lacy, "Gain at 185 nanometers in a laser-produced, photoionization-pumped indium plasma," Ph.D. dissertation (Stanford University, Stanford, Calif., 1987).

13. H. C. Gerritsen, H. van Brug, G. Bijkerk, and M. J. van der Wiel, "Laser-generated plasma as soft x-ray source," J. Appl. Phys. **59,** 2337–2344 (1986).

14. W. T. Silfvast, O. R. Wood II, and D. Y. Al-Salameh, "Direct photoionization pumping of high gain VUV, UV and visible inversions in helium, cadmium and argon via two-electron (shakeup) and of sodium via the output from the LLNL soft-x-ray laser," in *Short Wavelength Coherent Radiation: Generation and Applications*, D. T. Attwood and J. Bokor, eds., AIP Conf. Proc. **147,** 134–144 (1986).

15. R. W. P. McWhirter, "Spectral intensities," in *Plasma Diagnostic Techniques*, R. H. Huddlestone and S. L. Leonard, eds. (Academic, New York, 1965), Chap. 5, p. 206.

16. S. Basu and R. L. Byer, "Generation of 500-MW peak power pulses from an injection mode-locked Q-switched Nd:glass moving slab laser," in *Digest of Conference on Lasers and Electro-Optics* (Optical Society of America, Washington, D.C., 1988), paper ThV1.

17. T. Andersen, A. Kirkegård Nielsen, and G. Sørensen, "A systematic study of atomic lifetimes of levels belonging to the Ag I, Cd I, Au I, and Hg I isoelectronic sequences," Phys. Scr. **6,** 122–124 (1972).